ISSN 1392–1320 MATERIALS SCIENCE (MEDŽIAGOTYRA). Vol. 17, No. 2. 2011

Frequency Dependent Electrical Properties of Ferroelectric $Ba_{0.8}Sr_{0.2}TiO_3$ Thin Film

Ala'eddin A. SAIF *, Zul Azhar ZAHID JAMAL, Zaliman SAULI, Prabakaran POOPALAN

Microfabrication Cleanroom, School of Microelectronic Engineering, University Malaysia Perlis (UniMAP), BlockA3 SME Bank, Kuala Perlis, 02000 Perlis, Malaysia

Received 19 January 2011; accepted 02 May 2011

The frequency dependent electrical parameters, such as impedance, electric modulus, dielectric constant and AC conductivity for ferroelectric $Ba_{0.8}Sr_{0.2}TiO_3$ thin film have been investigated within the range of 1 Hz and 10^6 Hz at room temperature. Z^* plane shows two regions corresponding to the bulk mechanism and the distribution of the grain boundaries-electrodes process. M'' versus frequency plot reveals a relaxation peak, which is not observed in the ε'' plot and it has been found that this peak is a non-Debye-type. The frequency dependent conductivity plot shows three regions of conduction processes, i. e., a low-frequency region due to DC conduction, a mid-frequency region due to translational hopping motions and a high-frequency region due to localized hopping and/or reorientational motion.
Keywords: BST thin film; ferroelectric; impedance; dielectric properties; AC conductivity.

1. INTRODUCTION

For the past few years, barium strontium titanate (BST) has attracted considerable interest in many microelectronic applications such as ferroelectric field effect transistors (FeFET), dynamic access random memory (DRAM) [1] and infrared detectors [2] due to its high dielectric constant, low dielectric loss and relatively low leakage current. BST is a solid solution family composed of barium titanate and strontium titanate with Curie temperature covering a wide range of temperature [3, 4]. In BST when strontium ions are introduced at A sites of the ABO_3 perovskite matrix, many parameters will be effected such as the unit cell volume and Curie temperature [3], which in turn directly affects on the dielectric and conduction mechanism of BST. Between all BST family, $Ba_{0.8}Sr_{0.2}TiO_3$ shows relatively strong ferroelectric behavior with Curie temperature close to the room temperature [5], which gives it advantage over the rest of the BST family in many application, in particular, for uncooled infrared detectors [2].

Impedance spectroscopy has been extensively employed in electroceramics, due to its capabilities i) to resolve grain boundary from bulk electrical properties, ii) to calculate materials constants (conductivity and dielectric constant), and iii) to probe the electrical homogeneity [6]. Relatively, few studies reported the AC impedance spectroscopy for BST in thin film form. D. Czekaj et al [7] reported that for a homogenous and inhomogeneous BST film, a single depressed semicircle is observed. In the current work, sol-gel $Ba_{0.8}Sr_{0.2}TiO_3$ thin film is successfully fabricated as a metal-ferroelectric-metal (MFM) configuration. Different AC electrical parameters, such as impedance, electric modulus, dielectric constant and AC conductivity, are presented in order to correlate the nanostructure of the film with the conduction mechanism and dielectric relaxation phenomenon. The measurements were performed using an impedance/gain-phase analyzer in the frequency range of 1 Hz to 1 MHz at room temperature.

2. EXPERIMENT

$Ba_{0.8}Sr_{0.2}TiO_3$ solution was prepared using barium acetate, strontium acetate and titanium (IV) isopropoxide as starting material, the preparation details for the solution can be found elsewhere else [1].

$Ba_{0.8}Sr_{0.2}TiO_3$ solution was deposited on a $Pt/SiO_2/Si$ substrate via spin-coater at 5000 rpm for 20 seconds, followed by baking at 200 °C for 20 minutes and heating at 500 °C for 30 minutes in order to vaporize the organic solvent. The deposition and heating processes were repeated until the desirable thickness was obtained. Finally, the films were annealed at 800 °C for 1 hour in an O_2 atmosphere. The film thickness was measured using a stylus profilometer and it was found to be 450 nm.

The crystallization of the film was determined using an X-ray diffractometer (XRD) with a CuK_α radiation source (λ = 1.54 Å), operated at a voltage 40 KV and a current of 40 mA. The grain size was measured using atomic force microscope (AFM) (SPA400, SII Nanotechnology Inc.), operated in contact mode. For impedance measurement, dots of Al with an area of 7.85×10^{-3} cm^2 were deposited on top of the film as the top electrode using a shadow mask. The impedance and dielectric measurements were performed using an impedance gain/phase analyzer (Solartron 1260) in the frequency range of 1 Hz to 1 MHz at room temperature.

3. RESULTS AND DISCUSION

3.1. XRD and AFM analysis

Fig. 1, a, shows the XRD patterns of $Ba_{0.8}Sr_{0.2}TiO_3$ film annealed at 800 °C for 1 hour. It can be observed from the figure that the diffraction peaks are (100), (110), (111), (200), (210) and (211) within the 2θ range from 20° to 60°, furthermore, the measured a-axis and c-axis lattice

*Corresponding author. Tel.: +60-19-4948919; fax.: +604-9798305.
E-mail address: *alasaif82@hotmail.com* (A. A. Saif)

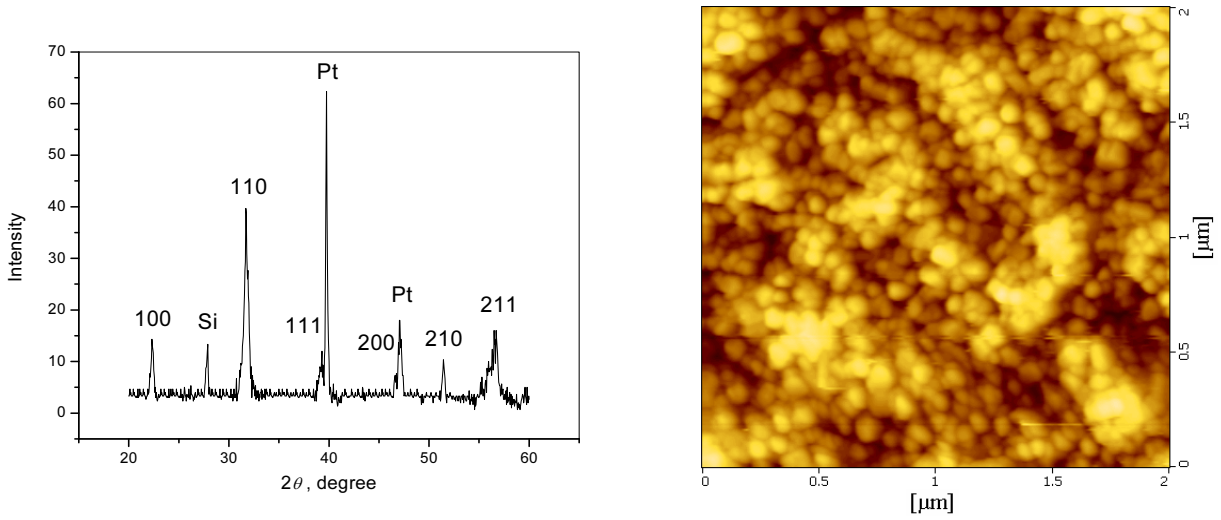

a b

Fig. 1. XRD patterns (a) and AFM micrograph (b) for $Ba_{0.8}Sr_{0.2}TiO_3$ film

parameters are 3.9805 Å and 4.0173 Å, respectively. This indicates that the film is crystallized with the tetragonal perovskite structure phase.

In order to measure the grain size for the film used in this work, AFM measurement was carried out for three different positions of an area of 2 μm × 2 μm. Fig. 1, b, shows a two dimensional AFM micrograph for the $Ba_{0.8}Sr_{0.2}TiO_3$ film, it can be seen from the figure that the surface quality of the film is relatively good; the average value of the grain size for the film is ~95 nm.

3.2. Ferroelectric analysis

In order to study the ferroelectric properties for the film used in this work, the capacitance–voltage (*C–V*) characteristics have been investigated using a Keithley 4200 semiconductor parameter analyzer. Fig. 2 shows the *C–V* characteristics for the film at 500 kHz and at room temperature.

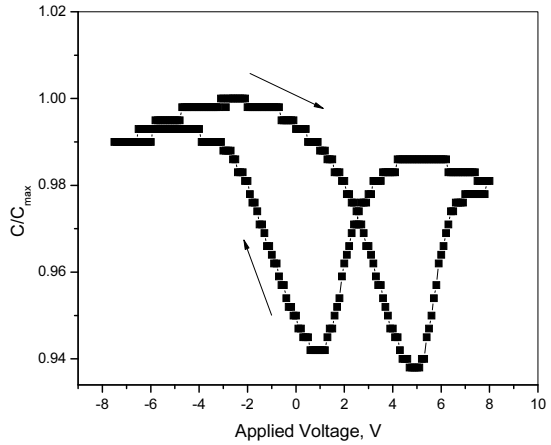

Fig. 2. The capacitance-voltage characteristics of $Ba_{0.8}Sr_{0.2}TiO_3$ film at room temperature

The capacitance was measured while a DC bias voltage was swept from –7.5 V to +7.5 V and then reversed, with a sweeping rate of 0.01 V/s. It is observed that the capacitance varies non-linearly with the applied voltage. However, a well defined butterfly-shape variation with two peaks of the capacitance is observed; these peaks are formed as a result of a spontaneous polarization switching [8], indicating that the film has a ferroelectric nature. Furthermore, an observed asymmetry and shift in the *C–V* curve toward the positive voltage range suggests that the films contain mobile negative ions or charges accumulated at the interface between the film and the electrode. In addition, there is a difference between the capacitance values of the two peaks, which may be due to some defect in energy levels in the film [9].

3.3. Impedance analysis

AC impedance spectroscopy has been proved to be a powerful method to estimate the contribution of the grain, grain boundaries and film/electrode effects on the charge transport phenomenon in perovskite materials [10]. The complex impedance $Z^*(f)$ of the BST system can be described by the following equation:

$$Z^*(f) = Z'(f) + jZ''(f), \quad (1)$$

where Z' and Z'' represent the real and imaginary part of impedance, respectively.

Fig. 3 (a) and (b) show the variation of the real (Z') and imaginary (Z'') components of the impedance with frequency for the tested film. The magnitude of Z' decreases with the increase of frequency, indicating an increase in AC conductivity of the film. The variation of Z'' with frequency reveals that Z'' values reach a maximum (Z''_{max}), showing a peak. Such behavior indicates the presence of relaxation in the system.

Fig. 4 shows the Nyquist plot of $Ba_{0.8}Sr_{0.2}TiO_3$ film. The plot shows a semicircular arc at high frequencies responding to the electrical properties of the bulk of the film. Whereas, at intermediate and low frequencies, the plot shows a depressed semicircle as a response to the grain boundaries and film/electrodes interface contributions to the polarization mechanism in this range of frequencies.

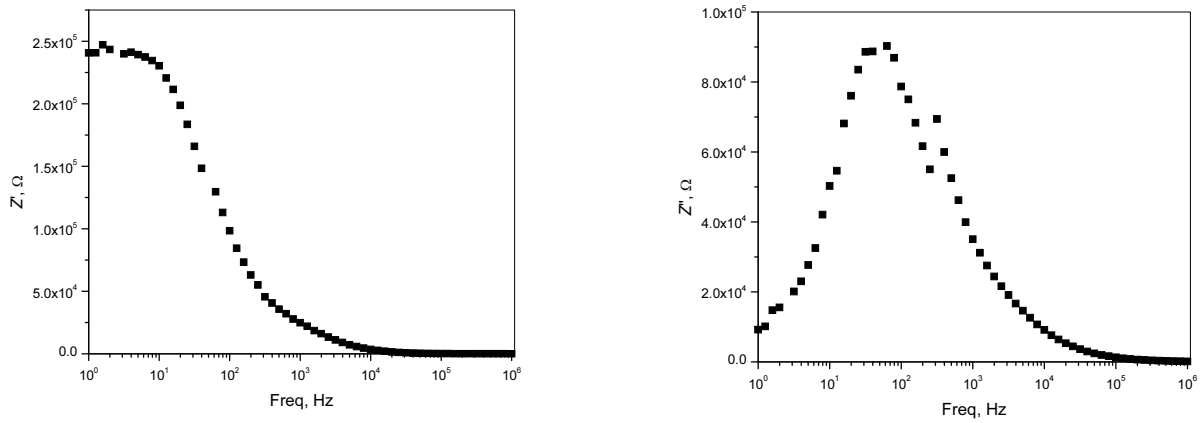

a b

Fig. 3. Variation of real (a) and (b) imaginary components of impedance as a function of frequency for $Ba_{0.8}Sr_{0.2}TiO_3$ film

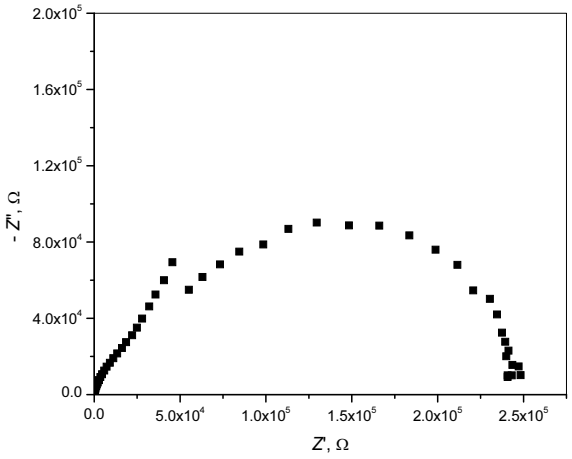

Fig. 4. Nyquist plots for $Ba_{0.8}Sr_{0.2}TiO_3$ film

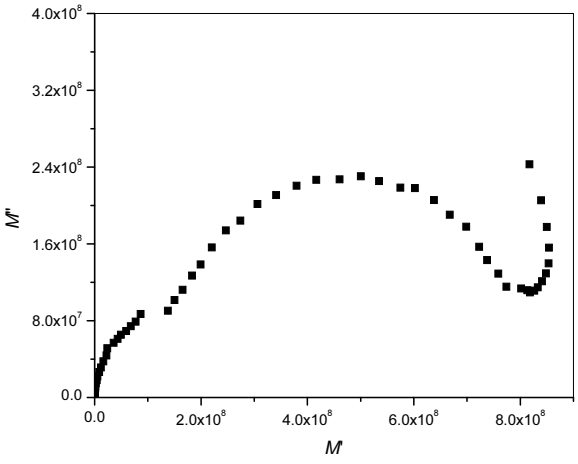

Fig. 5. Electric modulus planes for $Ba_{0.8}Sr_{0.2}TiO_3$ film

In order to resolve the overlapping of the conduction mechanisms for the bulk, grain boundaries, and film/electrode interfaces in the Nyquist plot, electric modulus planes of the film is plotted over the same frequency range as shown in Fig. 5. It can be observed that *M** plot has an inflexion, i. e., minimum value, at high frequencies; the small portion exists after this inflexion could be attributed to the bulk due to the frequency range and it appears in the Nyquist plot as a semicircular arc. Further increments in frequency are not possible due to hardware limits. In addition, the region between the origin and the inflexion, *M** shows a semicircular arc and depressed semicircle overlapped together, these features confirm that *Z** plot in this range of frequencies consists of two overlapped regions.

3.4. Dielectric analysis

The study of the dielectric properties is another important source of valuable information about conduction processes since it can be used to understand the origin of the dielectric losses, the electrical and dipolar relaxation time and its activation energy [11].

The dielectric permittivity was determined from the measured values of the impedance using the following relation [12]

$$\varepsilon^* = \varepsilon' + j\varepsilon'' = \frac{-Z'}{(Z'^2 + Z''^2)\omega C_o} + j\frac{-Z''}{(Z'^2 + Z''^2)\omega C_o}, \qquad (2)$$

where ε' and ε'' are the real and imaginary components of the dielectric permittivity, respectively.

Fig. 6 shows the frequency dependent plot of ε' for $Ba_{0.8}Sr_{0.2}TiO_3$ film. It is observed that the value of ε' decreases as the frequency increases and attains a constant limiting value ε'_∞. This can be explained according to the behavior of the dipoles movement, the dielectric permittivity related to free dipoles oscillating in the presence of an alternating electric field. At very low frequencies ($f < 1/\tau$, τ is the relaxation time), dipoles follow the electric field. As the frequency increases, dipoles begin to lag behind the field and ε' slightly decreases. When the frequency reaches the characteristic frequency ($f = 1/\tau$), the dielectric constant drops (relaxation process). At very high frequencies ($f > 1/\tau$), dipoles can no longer follow the field and $\varepsilon' \approx \varepsilon'_\infty$ [13]. The high values of dielectric constant at low frequencies can be explained as the accumulation of charges at the grain boundaries and at the interfaces

between the sample and the electrode, i. e., space charge polarization [14].

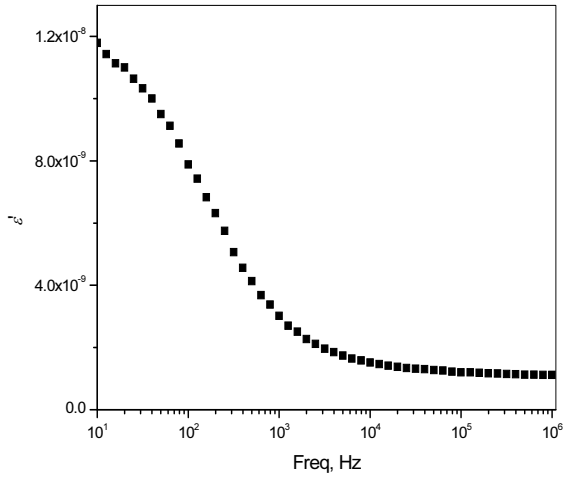

Fig. 6. Variation of ε' versus frequency for $Ba_{0.8}Sr_{0.2}TiO_3$ film at room temperature

Fig. 7 shows the frequency dependent of dielectric loss ε'' for the tested film at room temperature. The same feature for dielectric loss is observed as for dielectric constant. There are no appreciable relaxation peaks in the frequency range employed in this study. It is believed that the ionic conduction may mask any relaxation mechanism.

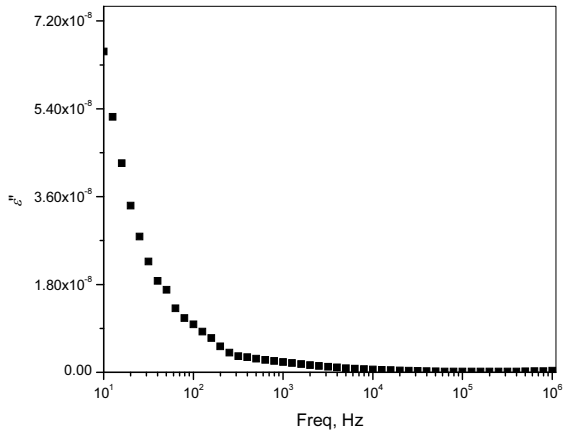

Fig. 7. Variation of ε'' versus frequency for $Ba_{0.8}Sr_{0.2}TiO_3$ film at room temperature

In order to reveal the relaxation peak in ε'' plot, the effect of the electrode polarization must be excluded. This can be achieved by following the electric modulus approach, since the electric modulus corresponds to the relaxation on the electric field in the material when the electric displacement remains constant. Fig. 8 shows the variation of M'' as a function of frequency. It can be seen that M'' shows a low and unclear peak at low frequency ~70 Hz attributed to the electrode effect, and a dominated peak located in the range of ~50 Hz to 1 kHz, attributed to the grain boundaries mechanism. The observed peaks in M'' plot can explain the arc and the well defined semicircle in the M^* plot.

The modulus plot can be characterized by full width at half height or in terms of a non-exponential decay function. The stretched exponential function is defined by the empirical Kohlrausch-Williams-Watts (KWW) relationship [15, 16].

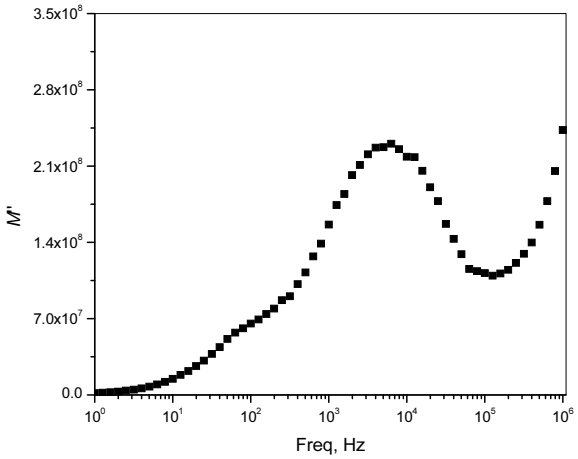

Fig. 8. Variation of the M'' versus frequency for $Ba_{0.8}Sr_{0.2}TiO_3$ film

$$\phi(f) = e^{(-t/\tau)^{\beta}} \qquad 0 < \beta < 1, \tag{3}$$

where τ is the characteristic relaxation time and β is the Kohlrausch parameter, which represents the deviation from a Debye-type relaxation ($\beta = 1$) and it decreases with the increasing of the relaxation time distribution.

The value of the parameter β is calculated by extracting FWHM of the modulus peaks using $\beta = 1.14/\text{FWHM}$. It has been found that the value of β for the tested film is 0.95. This indicates that the relaxation process for the current sample is of a non-Debye-type.

3.5. AC conductivity

The study of frequency dependent conductivity is a well-established method for characterizing the hopping dynamics of the charge carrier/ions. Fig. 9 shows a typical frequency dependence of AC conductivity σ for $Ba_{0.8}Sr_{0.2}TiO_3$ film.

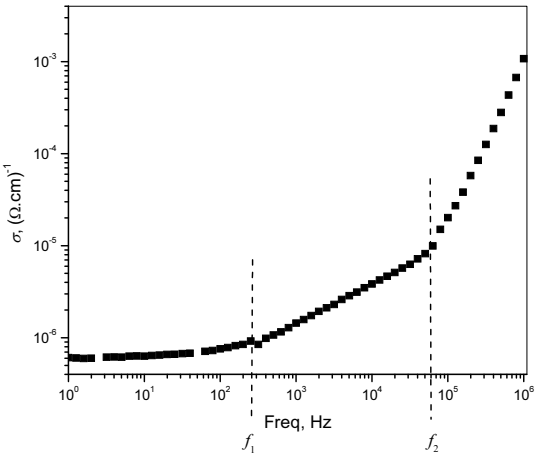

Fig. 9. AC conductivity σ (f) as a function of frequency for $Ba_{0.8}Sr_{0.2}TiO_3$ film at room temperature

The frequency dependence of AC conductivity is usually characterized by a power law as given below [17 – 20].

$$\sigma_{AC} = Af^n, \quad (4)$$

where A is a temperature-dependent constant and n is the frequency exponent, which can be determined from the measured results.

It is observed from Fig. 9 that the curve shows two threshold frequencies, f_1 and f_2, separating the entire variation into three regions: (i) Low frequencies region, $f < f_1$, in which the conductivity is almost frequency-independent, and called σ_{DC}. (ii) Moderate frequencies region, $f_1 < f < f_2$; the conductivity increases linearly with the frequency. The value of n is obtained by fitting σ versus f plots in this region, which is found to be 0.51, i. e. $0 < n < 1$. This reveals that the conduction mechanism in this region corresponds to the translational hopping motion [18, 20]. (iii) High frequencies region, $f > f_2$, as well the conductivity increases linearly with the frequency. In this region the n value is 1.77, i. e. $1 < n < 2$, which reveals that the conduction mechanism in this range of frequency corresponds to the well-localized hopping and/or reorientational motion [18, 20].

4. CONCLUSION

The frequency dependent electrical parameters, such as impedance, electric modulus, dielectric constant and AC conductivity for $Ba_{0.8}Sr_{0.2}TiO_3$ thin film have been investigated within the range of 1 Hz and 10^6 Hz. Z^* plane shows two regions corresponding to the bulk mechanism and the distribution of the grain boundaries-electrodes process. M'' versus frequency plot reveals a relaxation peak, which is not observed in the ε'' plot and it has been found that this peak is a non-Debye-type. The frequency dependent conductivity plot shows three regions of conduction processes, i. e., a low-frequency region due to DC conduction, a mid-frequency region due to translational hopping motions and a high-frequency region due to localized hopping and/or reorientational motion.

REFERENCES

1. **Saif, Ala'eddin A., Poopalan, P.** Electrical Properties of Metal-ferroelectric-insulator-semiconductor Structure using $Ba_xSr_{1-x}TiO_3$ for Ferroelectric-gate Field Effect Transistor *Solid-State Electronic* 62 (1) 2011: pp. 24 – 30.
2. **Cheng, J.-G., Tang, J., Zhang, A.-J., Meng, X.-J., Chu, J.-H.** Sol-gel-derived Pyroelectric Barium Strontium Titanate Thin Films for Infrared Detector Applications *Applied Physics A* 71 (6) 2000: pp. 667 – 670.
3. **Patil, D. R., Lokare, S. A., Devan, R. S., Chougule, S. S., Kanamadi, C. M., Kolekar, Y. D., Chougule, B. K.** Studies on Electrical and Dielectric Properties of $Ba_{1-x}Sr_xTiO3$ *Material Chemistry and Physics* 104 (2 – 3) 2007: pp. 254 – 257.
4. **Ngo, E., Nothwang, W. D., Hubbard, C., Hirsch, S., Cole, M. W., Chang, W., Kirchoffer, S. W., Pond, J. M.** $Ba_{1-x}Sr_xTiO3$ Ased Thin Films for Next Generation Devices, *Army Research Laboratory* 2004: Report Number: ARL-TN-228, Aberdeen Proving Ground, MD 21005-5069.
5. **Pontes, F. M., Leite, E. R., Pontes, D. S. L., Longo, E., Santos, E. M. S., Mergulha, S., Pizani, P. S., Lanciotti, F., Boschi, T. M., Varela, J. A.** Ferroelectric and Optical Properties of Thin $Ba_{0.8}Sr_{0.2}TiO_3$ Film *Journal of Applied Physics* 91 (9) 2002: pp. 5972 – 5978.
6. **Jin-Ha, H., Mason, T. O., Garboczi, E.** Electrical/ /Dielectric Properties of Nanocrystalline Cerium Oxide, in *Nanophase and Nanocomposite Materials II Materials Research Society* 457 1997: pp. 27 – 32.
7. **Czekaj, D., Lisinska-Czekaj, A., Orkisz, T., Orkisz, J., Smalarz, G.** Impedance Spectroscopic Studies of Sol-gel Derived Barium Strontium Titanate Thin Films *Journal of European Ceramic Society* 30 (2) 2010: pp 465 – 470.
8. **Li, G., Yu, P., Xiao, D.** Ferroelectric Properties of Ba_{1-x} Sr_x TiO_3 Thin Films Synthesized by Using Novel Sol-gel Technique Through Carbonates *Journal of Electroceramics* 21 (1 – 4) 2008: p. 340.
9. **Kumari, N., Krupanidhi, S. B., Varma, K. B. R.** Dielectric, Impedance and Ferroelectric Characteristics of c-oriented Bismuth Vanadate Films Grown by Pulsed Laser Deposition *Materials Science & Engineering B* 138 (1) 2007: pp. 22 – 30.
10. **Mahboob, S., Prasad, G., Kumar, G. S.** Impedance and a.c. Conductivity Studies on $Ba(Nd_{0.2}Ti_{0.6}Nb_{0.2})O_3$ Ceramic Prepared Through Conventional and Microwave Sintering route *Bulletin Material Science* 29 (4) 2006: pp. 347 – 355.
11. **Ayouchi, R., Leinen, D., Martin, F., Gabas, M., Dalchiele, E., Ramos-Barrado, J. R.** Preparation and Characterization of Transparent ZnO Thin Films Obtained by Spray Pyrolysis *Thin Solid Films* 426 (1 – 2) 2003: pp. 68 – 77.
12. **Dillip, K. Pradhan, R. N. P. Choudhary, B. Samantaray, K.** Studies of Dielectric Relaxation and AC Conductivity Behavior of Plasticized Polymer Nanocomposite Electrolytes *International Journal of Electrochemical Science* 3 2008: pp. 597 – 608.
13. **Tripathi, R., Kumar, A., Bharti, Ch., Sinh, T. P.** Dielectric Relaxation of ZnO Nanostructure Synthesized by Soft Chemical Method *Current Applied Physics* 10 (2) 2010: pp. 676 – 681.
14. **Sambasiva Rao, K., Murali Krishna, P., Madhava Prasad, D., Joon-Hyung, L., Jin-Soo, K.** Electrical, Electromechanical and Structural Studies of Lead Potassium Samarium Niobate Ceramics *Journal of Alloys and Compounds* 464 (1 – 2) 2008: pp. 497 – 507.
15. **Bing-Ce, L., Ci-Hui, L., Zhu-Xi, F., Bo, Y.** Effects of Grain Boundary Barrier in ZnO/Si Heterostructure *Chinese Physics Letter* 26 (11) 2009: pp. 117101-4.
16. **Song, S. H., Xiao, P.** An impedance Spectroscopy Study of Oxide Films Formed During High Temperature Oxidation of an Austenitic Stainless Steel *Journal of Materials Science* 38 (3) 2003: pp. 499 – 506.
17. **Anantha, P. S., Hariharan, K.** ac Conductivity Analysis and Dielectric Relaxation Behaviour of $NaNO_3$-Al_2O_3 Composites *Materials Science and Engineering B* 121 (1 – 2) 2005: pp. 12 – 19.
18. **Ram, M., Chakrabarti, S.** Dielectric and Modulus Studies on $LiFe_{1/2}Co_{1/2}VO_4$ *Journal of Alloys and Compounds* 462 (1 – 2) 2008: pp. 214 – 219.
19. **Dutta, A., Sinha, T. P., Jena, P., Adak, S.** Ac Conductivity and Dielectric Relaxation in Ionically Conducting Soda-Lime-Silicate Glasses *Journal of Non-Crystalline Solids* 354 (33) 2008: pp. 3952 – 3957.
20. **Akgul, U., Ergin, Z., Sekerci, M., Atici, Y.** AC Conductivity and Dielectric Behavior of $[Cd(phen)_2(SCN)_2]$ *Vacuum* 82 (3) 2008: pp. 340 – 345.